

Article

Radiation Modification of Optical Characteristics of LiNbO₃:Zn and LiNbO₃:Mg Crystals

Mikhail Palatnikov ¹, Nikolay Sidorov ^{1,*}, Sergey Panasjuk ², Natalya Teplyakova ¹ and Olga Makarova ¹ 

¹ Tananaev Institute of Chemistry-Subdivision of the Federal Research Centre, Kola Science Centre of the Russian Academy of Sciences, 184206 Apatity, Russia; m.palatnikov@ksc.ru (M.P.); n.teplyakova@ksc.ru (N.T.); o.makarova@ksc.ru (O.M.)

² St. Petersburg State Institute of Technology, Chemistry and Biochemistry Department, 190013 St. Petersburg, Russia; panasiuk.sergey1956@yandex.ru

* Correspondence: n.sidorov@ksc.ru or deenka@yandex.ru; Tel.: +7-8(81555)79-194

Abstract: The modification of the optical characteristics of LiNbO₃:Zn and LiNbO₃:Mg crystals grown by the Czochralski method was investigated using β and γ radiation. The photorefractive effect was found to be inhibited by ionizing radiation in the LiNbO₃:Zn ([ZnO] \approx 2.1 mol%) crystal, which belonged to a below-threshold concentration range. The inhibition was attributed to a stepwise radiation annealing of charged defects. Ionizing radiation increased the general optical uniformity of above-threshold crystals LiNbO₃:Zn ([ZnO] \approx 5.9 mol%) and LiNbO₃:Mg ([MgO] \approx 5.6 mol%). In addition, we determined that radiation annealing substantially influenced photorefractive dynamics in lightly doped LiNbO₃:Zn ([ZnO] \approx 0.1 mol%) crystals, which widens their application areas.

Keywords: lithium niobate; ionizing radiation; optical homogeneity; charged defects; photoinduced light scattering; conoscopic patterns



Citation: Palatnikov, M.; Sidorov, N.; Panasjuk, S.; Teplyakova, N.; Makarova, O. Radiation Modification of Optical Characteristics of LiNbO₃:Zn and LiNbO₃:Mg Crystals. *Crystals* **2022**, *12*, 600. <https://doi.org/10.3390/cryst12050600>

Academic Editor: László Kovács

Received: 11 March 2022

Accepted: 22 April 2022

Published: 25 April 2022

Publisher's Note: MDPI stays neutral with regard to jurisdictional claims in published maps and institutional affiliations.



Copyright: © 2022 by the authors. Licensee MDPI, Basel, Switzerland. This article is an open access article distributed under the terms and conditions of the Creative Commons Attribution (CC BY) license (<https://creativecommons.org/licenses/by/4.0/>).

1. Introduction

Ferroelectric lithium niobate (LN, LiNbO₃) crystals have attracted the attention of scientists working in integrated and nonlinear optics, acoustoelectronics, quantum electronics, and solid-state physics for many years [1–7]. LN crystals possess a photorefractive effect (optical damage); the effect value depends on the crystal's exact composition and secondary structure [6]. A number of recent pioneering works have been devoted to a noticeable change in the fundamentally important optical characteristics of LN crystals when they are doped with tetravalent cations [8–14]. Particularly impressive results are devoted to an increase in photorefractive in the UV region upon doping of LN crystals with alkaline earth metals and its suppression upon doping with tetravalent dopants. Interestingly, doping with tetravalent impurities at noticeably lower concentrations suppresses the photorefractive effect in the visible region more strongly than when doped, for example, with magnesium. Thus, the development of optical damage-resistant optically uniform LN-based materials has attracted the attention of scientists. It is an important task of modern materials science.

A number of LN crystal applications in optical devices can occur under the action of hard ionizing radiation. Thus, it is crucial to study the action of ionizing radiation on LN optical properties. Electronic defects can arise under the action of ionizing radiation; such defects determine the optical and electrical properties of LN crystals. A clear manifestation of the formation of defects in LN crystals is the appearance of color centers, where the centers contribute to the LN optical absorption.

Regarding this, radiation-induced defects also influence the photorefractive properties of the LN crystal, usually decreasing the optical damage resistance [15].

Our experience and the literature data [15] indicate that ionizing radiation should lead to an increase in the photorefractive sensitivity of LN crystals, decreasing its optical stability

and worsening its optical characteristics. We did not expect that ionizing radiation can suppress photorefraction in a below-threshold dopant concentrations range, for example, in the $\text{LiNbO}_3:\text{Zn}$ ($[\text{ZnO}] \approx 2.1$ mol%) crystal. Note that photorefraction in these crystals is not yet suppressed and laser beam destruction is observed. The results to be presented indicate that ionizing radiation can at least eliminate the destruction of the laser beam in the photoinduced laser scattering (PILS) pattern.

Ionizing radiation mostly excites secondary (interband) electrons in LN. Such electrons are located on different levels in a bandgap. This determines the formation of charged defects based on intrinsic and impurity point defects. The radiation of crystals leads to a restructuring of the existing defect structure, for example, re-charging of point defects (impurities, vacancies) [16]. Completely new defects appear only after the total recharge of all existing defects. In LN, the restructuring of the intrinsic defect structure is the nonequilibrium recharge of multivalent transition metal cations (for example, $\text{Fe}^{3+} \rightarrow \text{Fe}^{2+}$, $\text{Cu}^{2+} \rightarrow \text{Cu}^+$, etc.), and the formation of small-radii polarons and bi-polarons based on antisite Nb_{Li} and $\text{Nb}_{\text{Li-Nb}_{\text{Nb}}}$ defects [17].

Nonphotorefractive cations (Zn, Mg) increase the optical damage resistance [6] and introduce changes into the electronic subsystem of LN crystals. Nonphotorefractive cations (Zn, Mg, etc.) have constant valence. Unlike multivalent photorefractive cations (Fe, Rh, etc.), they are not electron donors, as they do not change their charge state under the optical radiation. This is why it is especially interesting to study ionizing radiation action on LN crystals doped with nonphotorefractive cations. Radiation defects are created and annealed under the action of radiation. The radiation dose absorbed by the differently doped crystals is sequentially accumulated. It is important to study how the creation of radiation-induced defects and dopant concentration influence optical uniformity and the photorefraction dynamics of LN crystals.

Doping causes abrupt changes on the properties of LiNbO_3 crystals [6,18,19], which is defined by the term "concentration threshold". Threshold concentration is such a concentration at which the defective structure, and physicochemical and optical characteristics of crystals change sharply [6,18,19]. The structure of the melt and the mechanism of incorporation of doping cations into the crystal structure change significantly when the doped LiNbO_3 crystal reaches threshold concentrations. In $\text{LiNbO}_3:\text{Zn}$ crystals, the threshold is near 5.2 mol% ZnO [18,19] and in $\text{LiNbO}_3:\text{Mg}$, near 5.5 mol% MgO [6]. Rearrangement of the crystal structure does not affect the space symmetry group of its unit cell even at dopant concentrations much higher than the threshold.

The article considers the influence of ionizing radiation on optical characteristics of Zn- and Mg-doped LN without discussing the photorefractive properties in detail. The paper studies crystals from the point of view of the creation of radiation-induced defects. The paper considers the connection between exact changes in the optical characteristics and dopant concentration of studied crystals. In this paper, we apply absorption spectroscopy, photoinduced light scattering (PILS), and laser conoscopy to compare optical characteristics of doped $\text{LiNbO}_3:\text{Zn}$ and $\text{LiNbO}_3:\text{Mg}$ crystals before and after β - and γ -radiation.

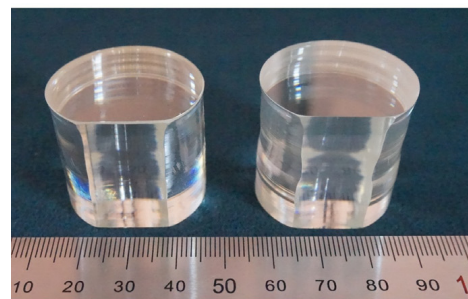
2. Materials and Methods

$\text{LiNbO}_3:\text{Mg}$ crystals were grown by the Czochralsky method along the polar axis from a melt of congruent composition. The melt contained 48.6 mol% Li_2O . Crystals were grown from platinum crucibles 75 mm in diameter. The axis gradient was low (1–2 deg/cm along the polar axis), the rotation speed was (18–20 rpm), and the pulling speed was low (0.75 mm/h). The growing speed was 1.04–1.08 mm/h. Crystals were grown on a plant Crystal-2 (ZavodKristall Ltd., Moscow, Russia) equipped with an automatic crystal diameter control system (Figure 1a). Before the beginning of growth, the melt was soaked for 8–11 h at a temperature 180–200 °C higher than the LN melting temperature (T_{melt}). This was performed to homogenize dopants and impurities in the melt. The thermal unit design was with double "insulation". Such a design provided an isothermal zone in the volume of the platinum screen for the after-growth annealing. Due to the thermal unit

design, $\text{LiNbO}_3\text{:Zn}$ and $\text{LiNbO}_3\text{:Mg}$ crystals were grown at a low-temperature gradient at a crystallization front. The thermal unit design was an analog to the one described in [20]. The boules diameter was 34–36 mm, and the cylindrical part length was 40 mm (Figure 1b).



a



b

Figure 1. A plant Crystal-2 for growing of LN crystals by Czochralsky method (a); $\text{LiNbO}_3\text{:Zn}$ and $\text{LiNbO}_3\text{:Mg}$ crystals (b).

After growth, $\text{LiNbO}_3\text{:Zn}$ and $\text{LiNbO}_3\text{:Mg}$ crystals were annealed in the plant at $1200\text{ }^\circ\text{C}$ for 10 h, and then cooled with a speed 50 deg/h . A long after-growth annealing under the platinum screen [20] is necessary for homogenization of the doped crystal composition and removal of thermal and mechanical stresses.

Charge was synthesized using niobium pentoxide Nb_2O_5 (Russian technical condition 1763-025-00545484-2000, Solikamsk, Russia) and lithium carbonate Li_2CO_3 (less than $3 \cdot 10^{-4}\text{ wt\%}$ impurities). A granular charge of congruent composition ($[\text{Li}_2\text{O}] = 48.6\text{ mol\%}$) was obtained from these initial components by the method of synthesis-granulation; the charge had a high bulk density (3.4 g/cm^3). The dopant was added as oxides (ZnO or MgO) with impurities not more than $5 \cdot 10^{-4}\text{ wt\%}$. The mixture was thoroughly mixed.

LN crystals were turned to a single domain state by high-temperature electro-diffusion annealing. A constant direct current was applied to polar cuts of the crystal during its cooling with the 20 deg/h speed. The current was applied in the temperature range of $1210\text{--}870\text{ }^\circ\text{C}$. Methods such as doping, growing, and turning to a single-domain state are described in detail in works [18–20].

Absorption spectra, PILS, and conoscopic patterns were studied using LN samples. The samples were cut from the middle of a cylindrical part of the crystal boule as cuboids $6 \times 7 \times 8 \text{ mm}^3$. Edges of the cuboids coincided with crystallographic axes. Faces of the cuboids were thoroughly polished. Dopant concentrations were determined in plates cut from the top (cone, C_{top}) and bottom (C_{bot}) parts of the boule. Elements concentrations were determined by AES at ICPE-9000 (Shimadzu, Kyoto, Japan). The dopant concentration in the crystal was determined as an average, $(C_{\text{top}} + C_{\text{bot}})/2$. Four LN:Zn crystals ($[\text{ZnO}] = 0.1, 2.1, 5.2, 5.9 \text{ mol\%}$) and one LN:Mg crystal ($[\text{MgO}] = 5.6 \text{ mol\%}$) were grown for this paper.

A laser Nd:YAG (MLL-100, Changchun New Industries Optoelectronics, Changchun, China) ($\lambda = 532 \text{ nm}$, I up to $\sim 6.29 \text{ W/cm}^2$) was used in experiments on PILS and laser conoscopy. The radiation scattered by the crystal was incident on a semitransparent screen placed behind the crystal and recorded by a digital video camera. In PILS experiments, the laser beam was directed along the y axis, and the electric field strength vector E of the laser radiation was parallel to the polar z axis of the crystal. In laser conoscopy studies, the sample was installed on a movable two-coordinate optical stage. This made it possible to obtain a plurality of conoscopic patterns corresponding to different parts of the cross-section of the sample. The conoscopic pattern was recorded on a translucent screen with a digital camera. A more detailed description of the methods for studying PILS and laser conoscopy in widely divergent laser beams, as well as block diagrams of experimental setups, is presented in [20].

$\text{LiNbO}_3\text{:Zn}$ and $\text{LiNbO}_3\text{:Mg}$ crystals samples were irradiated at room temperature by a β radiation source with radionuclides Sr-90+Y-90 type BIS-20 and an activity of $6.9 \times 10^{10} \text{ Bq}$. The maximum energy in the spectrum of beta particles was 2.26 MeV. The crystals were γ -irradiated using a MPX- γ -20 setup (Izotop, Nizhny Novgorod, Russia) from a Co^{60} source. The dose rate of γ -radiation was 0.5 Gy/s. The radiation dose was 20–40 kGy.

The absorbed dose rate of the source was determined using a ferrosulfate dosimeter. The dose D absorbed by the crystal was determined by the formula

$$D = (PS_{\text{cr}}/S_{\text{dos}})((Z/A)_{\text{cr}}/(Z/A)_{\text{dos}})t,$$

where P —dosage power according to ferrosulfate dosimeter (150 Gy/h); S_{cr} and S_{dos} —irradiated areas of the crystal and dosimeter, respectively; Z/A_{cr} and Z/A_{dos} —ratio of the effective atomic number to the effective atomic mass of an LN crystal (0.4599) and a ferrosulfate dosimeter (0.5525); t —exposure time.

Optical spectra were measured on an automatic spectrophotometer Specord M40 (Carl Zeiss Industrielle Messtechnik GmbH, Oberkochen, Germany) with a linear sweep over the wavenumber. The transmission spectra were measured in the range of 50,000–11,000 cm^{-1} (250–900 nm), and then they were recalculated into absorption spectra. During the irradiation and measurement of optical spectra, the flux of beta particles of the source and the light beam of the spectrophotometer were directed into the same plane (001) of the crystalline sample.

3. Results and Discussion

The study was started by the investigation of radiation-induced changes in LN:Zn and LN: Mg crystals [21]. The change in the optical transmission of $\text{LiNbO}_3\text{:Zn}$ (~ 0.04 – 5.9 mol\% ZnO in a crystal) crystals under ionizing radiation significantly and nonmonotonically depends on the zinc concentration [22]. This is due to the concentration thresholds. The latter are associated with the rearrangement of the crystal structure [6,18,19].

LN is a wide-gap dielectric with an uncontrolled set of small electron traps. It is clear that interpretation for radiation effects in such a crystal is difficult. An increase in optical absorption upon ionizing radiation occurs in a wide wavelength range of ~ 350 – 700 nm with a maximum change near ~ 400 – 450 nm [22]. The correct interpretation of this phenomenon

is also very difficult, as the LN optical spectra in this wavelength range contain a number of wide overlapping absorption bands [23].

In $\text{LiNbO}_3\text{:Zn}$ crystals with a dopant concentration near or above the concentration thresholds, the photorefractive effect is significantly suppressed [18,19], and laser beam destruction is not observed. At the same time, a significant photorefractive response is observed in LN:Zn crystals with below-threshold dopant concentrations ($[\text{ZnO}] \leq 3 \text{ mol\%}$), and the laser beam is strongly destroyed [18,19]. The main acceptor centers are antisite defects Nb_{Li} and random impurities of transition metals (including Fe), which inevitably exist in LN crystals. They act as electron traps in crystals doped below the concentration threshold, which is probably the main reason for the enhancement of the photorefractive response in below-threshold crystals. For example, iron ions recharge ($\text{Fe}^{3+} + e^- = \text{Fe}^{2+}$) or polarons form when an Nb_{Li} antisite defect captures an electron.

At threshold and above-threshold concentrations ($[\text{ZnO}] \geq 5.2 \text{ mol\%}$) [18,19], the ionizing radiation action of the LN crystal drastically changes. Occasional impurity cations Fe^{3+} localize in Nb sites [24]. It is obvious that the $[\text{Fe}^{3+}\text{Nb}]^{2-}$ center with an effective charge of -2 cannot be an electron trap and participate in the photorefractation process. At the same time, antisite defects Nb_{Li} are almost absent from threshold and above-threshold crystals [6,18].

This theory matches the recent views on the LN defective structure [25,26]: photorefractation decreases upon doping due to a decrease in antisite Nb_{Li} defects and weak polaron effects. We believe that the threshold nature of LN doping has a more complex reason. Restructuring is more complex at doping by both alkaline earth [15,18] and rare earth (REE) elements [20,27,28]. Doping by REE suppresses photorefractation in LN crystals. LN doped by REE (Er, Tb) has a significant number of niobium vacancies; niobium also occupies vacant sites of a perfect LN structure. REE cations substitute niobium cations in vacant positions as the REE concentration increases [27,28].

Thus, below-threshold LN:Zn ($[\text{ZnO}] \leq 3 \text{ mol\%}$) crystals have not only an increased photorefractation, but also a decreased optical transmission after ionizing radiation treatment [18,19,22].

The crystal $\text{LiNbO}_3\text{:Zn}$ (2.1 mol% ZnO) belongs to this concentration range. It has a number of charged defects, which also determine the photorefractive effect [18]. This is why radiative defect annealing in it has a stepwise character (Figure 2). It is believed [15] that radiation-induced defects should increase the photorefractive sensitivity of LN crystals. It is important to note that photorefractation is not yet suppressed and the destruction of the laser beam is observed (Figure 3a) in a range of below-threshold $\text{LiNbO}_3\text{:Zn}$ crystals. Thus, it was highly unexpected that ionizing radiation can suppress photorefractation of such a crystal, or at least eliminate laser beam destruction on a PILS pattern (Figure 3b).

Usually, in crystals with a suppressed photorefractation, PILS patterns do not change in time, and laser beam in them stays intact. The photorefractive response is absent, and the PILS indicatrix does not open, only a round scattering on static defects is observed (Figure 3b). The larger the diameter of the laser beam and the area of scattering, the lower the optical uniformity of the crystal. Crystals with a strong photorefractive effect have a tree-layered speckle-structured PILS pattern; it changes in time, and sometimes the changes are significant (Figure 3a). In time, the PILS shape changes from a circle (at the first second) into an oval (comet-shape). After that, the PILS indicatrix takes the shape of an asymmetric "eight" oriented along the polar axis (Figure 3a). The biggest PILS "petal" is oriented along the positive axis' direction, the smallest—along the negative one. All this is connected with a system of laser-induced dynamic defects; the defects are local changes in the refractive index of the crystal. Such PILS patterns indicate a very high photorefractive effect value in an LN crystal.

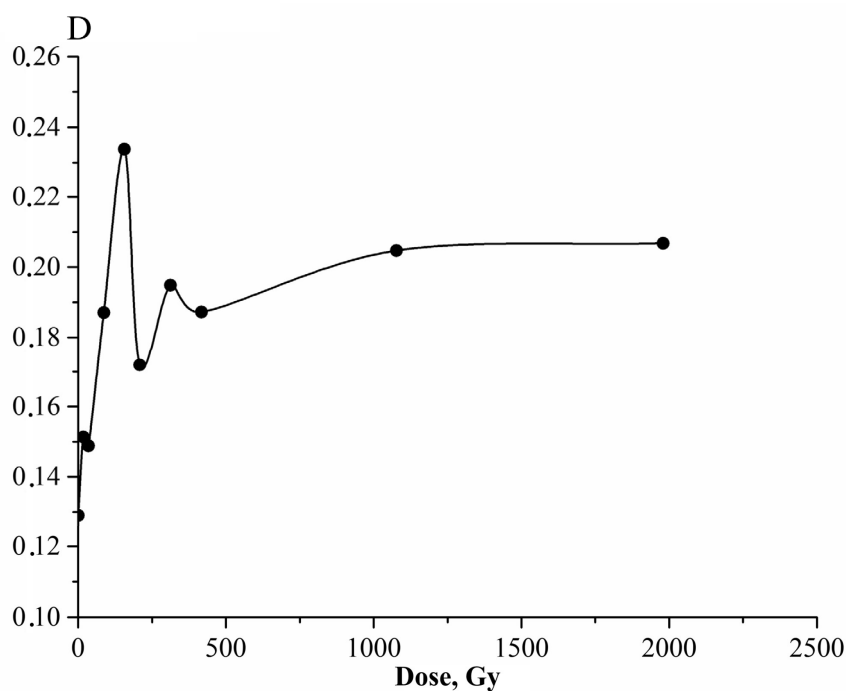


Figure 2. Dependence of optical density of LiNbO₃:Zn ([ZnO] ≈ 2.1 mol%) crystal on β radiation dose at λ = 420 nm.

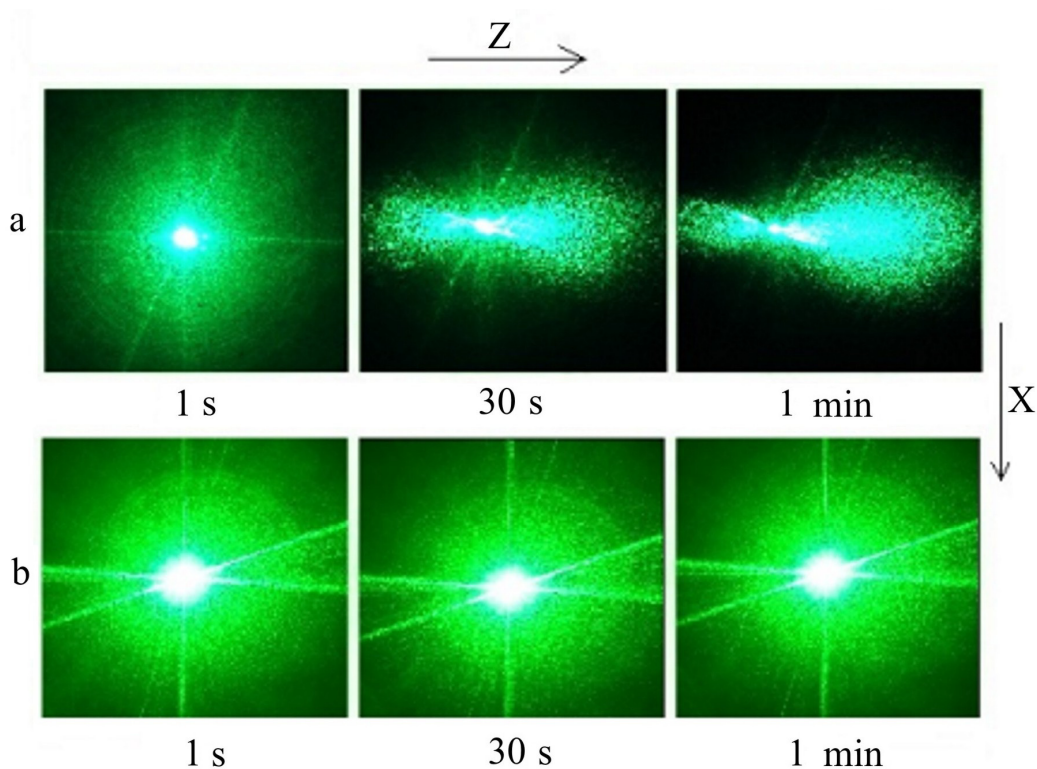


Figure 3. Pils patterns of LiNbO₃:Zn ([ZnO] ≈ 2.1 mol%) crystal before ionizing radiation treatment (a) and after β radiation with a 2.0 kGy dose (b). λ = 532 nm. P = 6.29 W/cm².

First, the charged defects concentration increases in a LiNbO₃:Zn (2.1 mol% ZnO) crystal under ionizing radiation action. Thus, the optical density of the crystal increases. However, as the dose accumulates, the charged defects amount decreases, and they are annealed by radiation and the optical density decreases (Figure 2). As the crystal has several

types of charged defects, the process repeats and goes in steps. Dynamic equilibrium is achieved at a certain ionizing radiation dose (radiation saturation dose).

LN crystals exhibit a consistent rearrangement of intrinsic defective structure, caused by the excitation of interband electrons. In this case, the suppression of photorefraction under the action of ionizing radiation is apparently caused by the super-equilibrium filling of deep electron traps (for example, $\text{Nb}_{\text{Li}} + e^-$ or $\text{Fe}^{3+} + e^- \rightarrow \text{Fe}^{2+}$), i.e., suppression occurs due to the nonequilibrium recharge of multivalent transition metal ions and the formation of polarons and bipolarons based on Nb_{Li} antisite defects. Next, the saturation of the radiation color of the crystals occurs with the successive accumulation of the radiation dose absorbed by the crystal (Figure 2). Defects in $\text{LiNbO}_3:\text{Zn}$ and $\text{LiNbO}_3:\text{Mg}$ crystals obviously continue to form under the action of ionizing radiation, but the rate of their formation is equal to the annihilation rate. The suppression of photorefraction in $\text{LiNbO}_3:\text{Zn}$ crystals occurs when the radiation color saturation dose is reached. The destruction of the laser beam is clearly observed in the $\text{LiNbO}_3:\text{Zn}$ crystal ($[\text{ZnO}] \approx 2.1 \text{ mol}\%$) before irradiation (Figure 3a), and disappears after irradiation (Figure 3b). This phenomenon is typical for $\text{LiNbO}_3:\text{Zn}$ crystals with a relatively low dopant concentration ($[\text{ZnO}] \leq 3 \text{ mol}\%$). Their photorefractive effect is clearly manifested before irradiation (Figure 3a).

The LN:Zn ($[\text{ZnO}] \geq 5.2 \text{ mol}\%$) crystal is on the very edge of the main threshold [18,19]. The effect of photorefraction is suppressed in it, and at least the laser beam remains intact (Figure 4b). The number of charged defects types in it is much less than in a $\text{LiNbO}_3:\text{Zn}$ (2.1 mol% ZnO) crystal [18,19]. This is why stepwise changes in optical transmission are not observed in it after ionizing radiation treatment (Figure 4a) [22].

PILS patterns of the $\text{LiNbO}_3:\text{Zn}$ ($[\text{ZnO}] = 5.2 \text{ mol}\%$) crystal show (Figure 4b) that the observed general optical uniformity does not change after ionizing radiation treatment of threshold crystals. At the same time, ionizing radiation treatment influences the optical uniformity of above-threshold crystals $\text{LiNbO}_3:\text{Zn}$ (~5.9 mol% ZnO) and $\text{LiNbO}_3:\text{Mg}$ (~5.6 mol% MgO) (Figures 5a and 6b) [6,18,19]. In addition, optical absorption does not change in $\text{LiNbO}_3:\text{Zn}$ ($[\text{ZnO}] > 5.2 \text{ mol}\%$) crystals even after high-ionizing-radiation doses [22]. For example, optical absorption does not change in an above-threshold crystal $\text{LiNbO}_3:\text{Zn}$ (~5.9 mol% ZnO) even at a sum β radiation dose of 13.6 kGy and γ radiation dose of 20 kGy (Figure 5b). The restructuring of the LN crystal structure near the concentration threshold not only suppresses photorefractive effects, but also leads to a total radiation resistance.

Ionizing radiation treatment increases the general optical uniformity of an above-threshold $\text{LiNbO}_3:\text{Zn}$ (~5.9 mol% ZnO) crystal. For example, PILS patterns of the $\text{LiNbO}_3:\text{Zn}$ crystal ($[\text{ZnO}] \approx 5.9 \text{ mol}\%$) clearly demonstrate a general decrease in the area of laser radiation scattered by static structural defects and focusing of the laser beam with the accumulation of the absorbed ionizing radiation dose (Figure 5).

The optical homogeneity also increases upon irradiation of heavily doped above-threshold $\text{LiNbO}_3:\text{Mg}$ crystals ($[\text{MgO}] \approx 5.6 \text{ mol}\%$) with ionizing radiation. This is confirmed by laser conoscopy and PILS data (Figures 6 and 7).

Both conoscopic patterns of an unirradiated $\text{LiNbO}_3:\text{Mg}$ crystal ($[\text{MgO}] \approx 5.6 \text{ mol}\%$) show signs of anomalous optical biaxiality: the Maltese cross stretches in the vertical direction, and the isochrones acquire some ellipticity but retain their integrity. In addition, there are defects on the upper left and lower left branches of the Maltese cross (Figure 6c). The contrast of conoscopic patterns (at 1 and 90 mW) of an unirradiated $\text{LiNbO}_3:\text{Mg}$ crystal ($[\text{MgO}] \approx 5.6 \text{ mol}\%$) is reduced compared to the conoscopic patterns of the same $\text{LiNbO}_3:\text{Mg}$ crystal ($[\text{MgO}] \approx 5.6 \text{ mol}\%$) after irradiation. At the same time, the image is blurrier, especially in the conoscopic pattern obtained with a laser radiation power of 1 mW (Figure 6). The observed anomalies in the conoscopic patterns are obviously associated with defects in the structure of the unirradiated $\text{LiNbO}_3:\text{Mg}$ crystal ($[\text{MgO}] \approx 5.6 \text{ mol}\%$). Defects reduce its optical uniformity. After irradiation of a $\text{LiNbO}_3:\text{Mg}$ crystal ($[\text{MgO}] \approx 5.6 \text{ mol}\%$), at a laser radiation power of 1 and 90 mW, the conoscopic patterns are standard. Such

patterns are characteristic of an optically uniaxial crystal. This feature indicates a higher optical uniformity of the studied crystal (Figure 6b).

PILS patterns confirm a general increase in optical uniformity of a $\text{LiNbO}_3:\text{Mg}$ ($[\text{MgO}] \approx 5.6 \text{ mol\%}$) crystal (Figure 7). The area of scattering on static defects decreases after ionizing radiation treatment as in the $\text{LiNbO}_3:\text{Zn}$ ($[\text{ZnO}] \approx 5.9 \text{ mol\%}$) crystal (Figures 5 and 7).

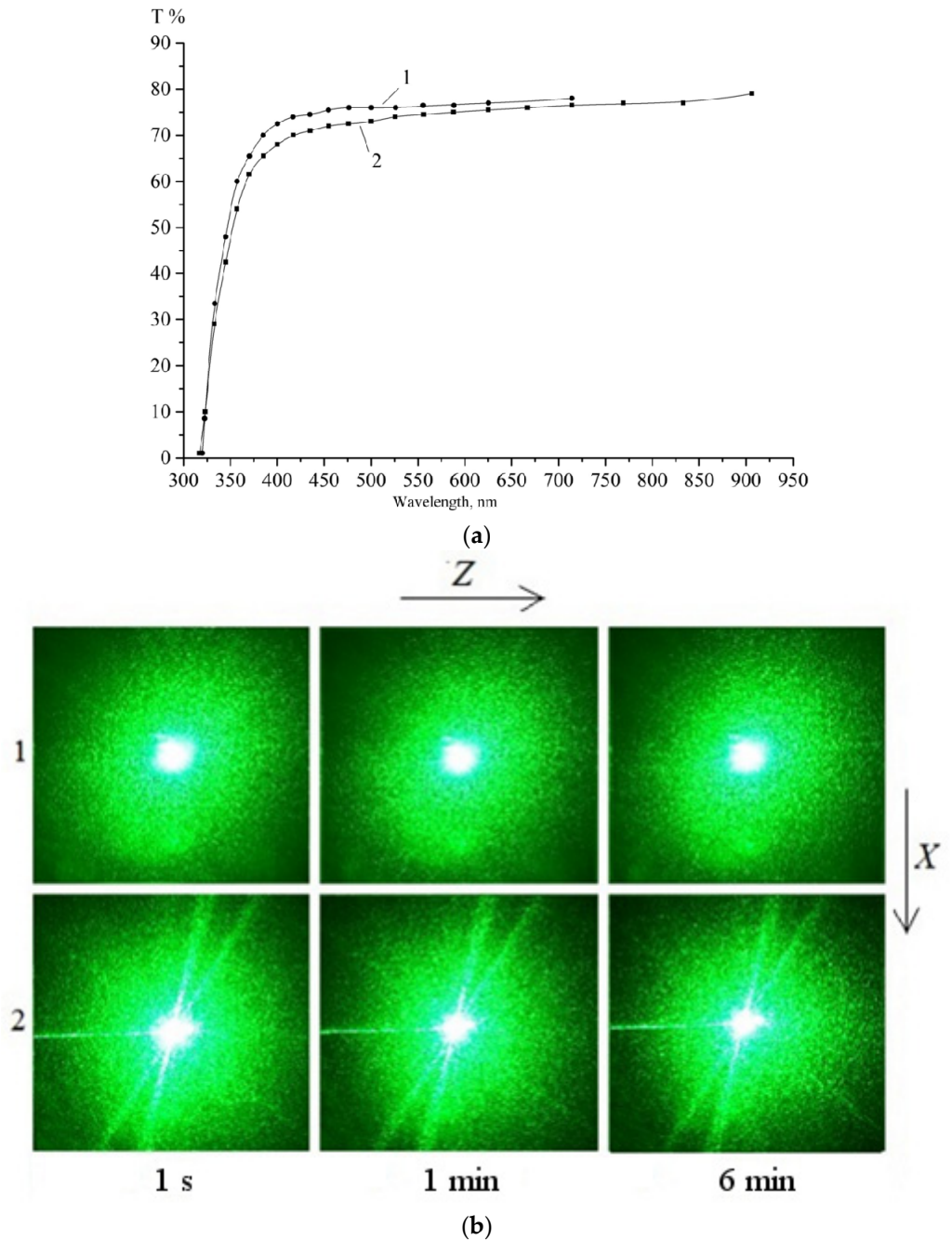


Figure 4. Optical transmission (a) and PILS patterns, $\lambda = 532 \text{ nm}$, $P = 6.29 \text{ W/cm}^2$ (b) of the crystal $\text{LiNbO}_3:\text{Zn}$ ($[\text{ZnO}] = 5.2 \text{ mol\%}$): 1—untreated, 2—treated with β radiation dose 10 kGy and γ radiation dose 8 kGy.

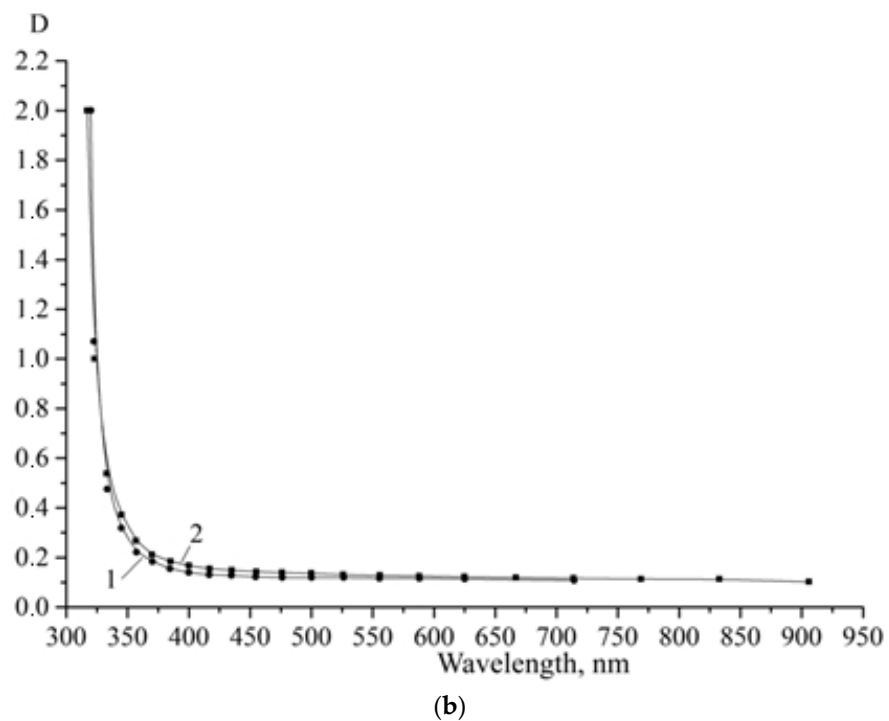
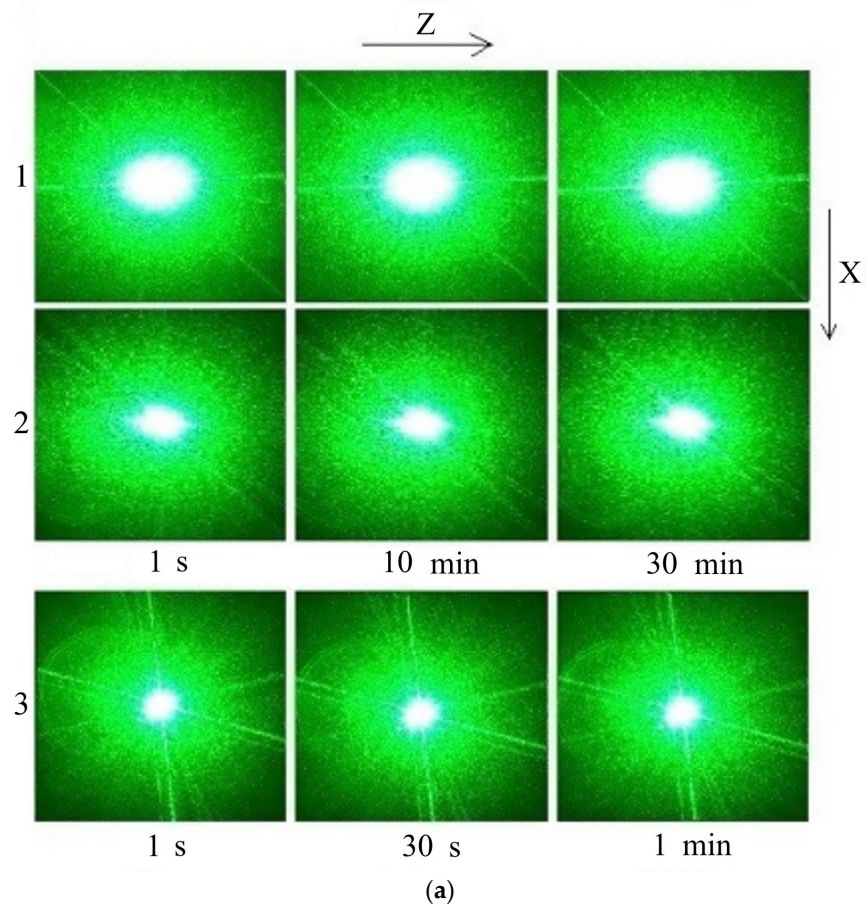


Figure 5. In the $\text{LiNbO}_3:\text{Zn}$ ($[\text{ZnO}] \approx 5.9 \text{ mol\%}$) crystal: (a) PILS patterns ($\lambda = 532 \text{ nm}$, $P = 6.29 \text{ W/cm}^2$) before ionizing radiation treatment (1), after γ radiation with a 2.0 kGy dose (2), and after additional β radiation with a 13.6 kGy and γ radiation with a 20.0 kGy dose (3); (b) absorption spectra before ionizing radiation treatment (1), and after β radiation with a 13.6 kGy and γ radiation with a 20.0 kGy dose (2).

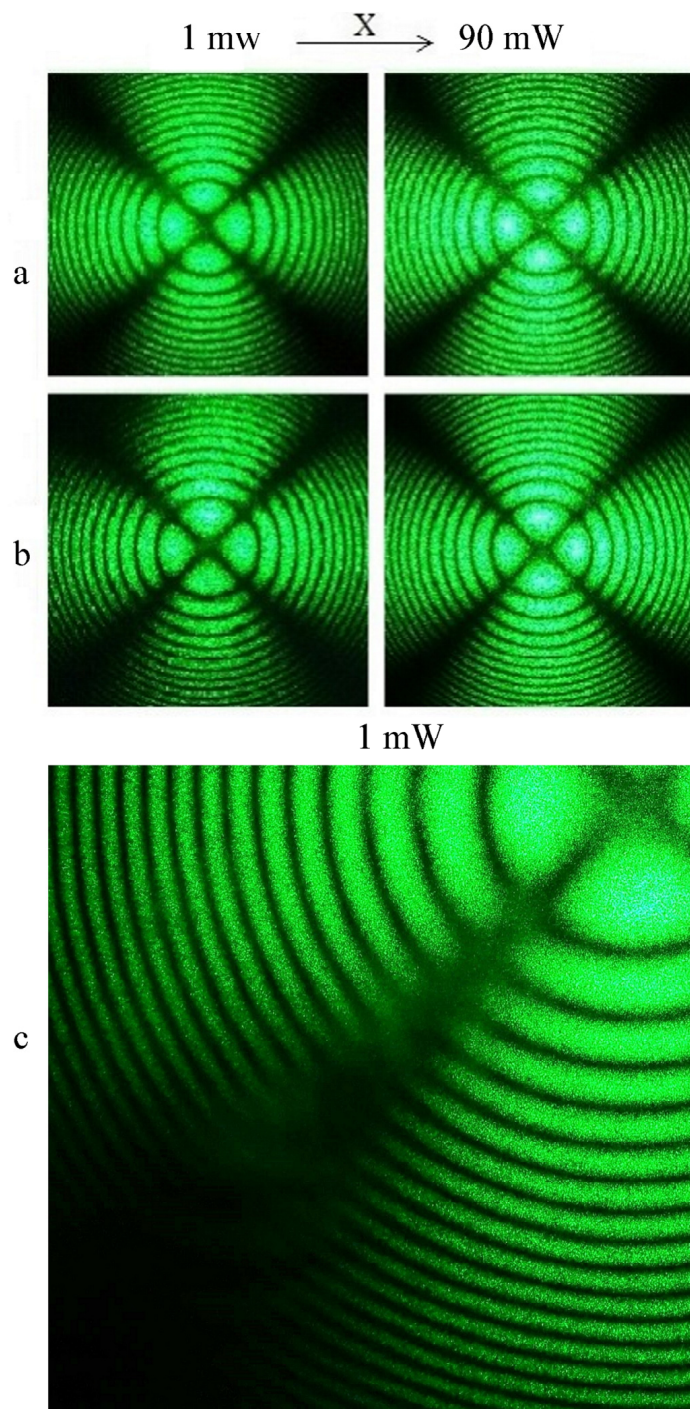


Figure 6. Conoscopic patterns of LiNbO₃:Mg ([MgO] \approx 5.6 mol%) crystal before ionizing radiation treatment (a); after γ radiation with a 5.0 kGy dose (b); Maltese cross fragment of the crystal before radiation (c). $\lambda = 532$ nm. P = 1 and 90 mW.

Probably, the optical homogeneity of heavily doped LiNbO₃:Zn and LiNbO₃:Mg crystals increases due to radiation annealing of charged structural defects and mechanical stresses. However, it is currently impossible to unambiguously interpret the observed phenomenon.

Interesting results are obtained in the study of LiNbO₃:Zn crystals with very low dopant concentrations ([ZnO] \approx 0.04–0.2 mol%). These crystals are close in composition to nominally pure LiNbO₃ crystals of congruent composition and have a pronounced photorefractive effect (Figure 8).

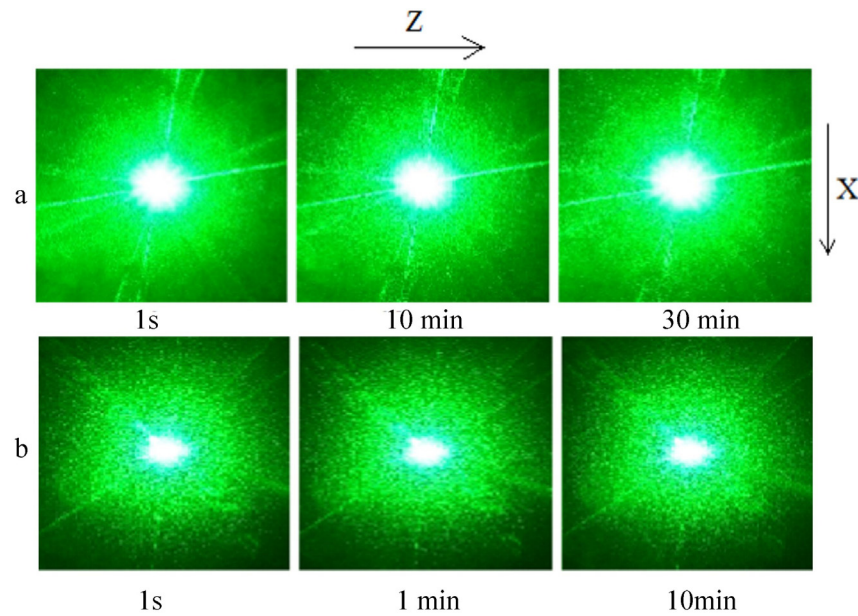


Figure 7. PILS patterns of $\text{LiNbO}_3\text{:Mg}$ ($[\text{MgO}] \approx 5.6 \text{ mol\%}$) crystal before ionizing radiation treatment (a) and after γ radiation with a 5.0 kGy dose (b). $\lambda = 532 \text{ nm}$. $P = 6.29 \text{ W/cm}^2$.

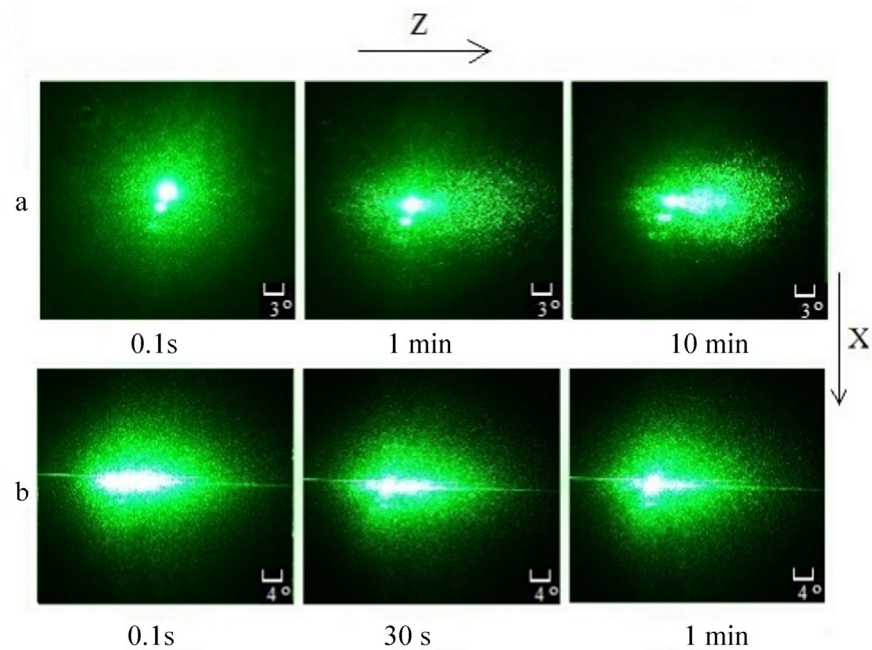


Figure 8. PILS patterns of $\text{LiNbO}_3\text{:Zn}$ ($[\text{ZnO}] \approx 0.1 \text{ mol\%}$) crystal before ionizing radiation treatment (a) and after β radiation with a 1.0 kGy dose (b). $\lambda = 532 \text{ nm}$. $P = 0.5 \text{ W/cm}^2$.

After ionizing radiation treatment, the PILS indicatrix speckle structure opens very quickly in such crystals, even at relatively low powers of exciting laser radiation ($P = 0.5 \text{ W/cm}^2$). This occurs within less than 0.1 seconds after the start of laser irradiation of the crystal (Figure 8a). Before irradiation, the indicatrix of the PILS speckle structure opens for about a minute in the same crystal (Figure 8b). We assume that the effect is caused by above-equilibrium filling of shallow electron traps under ionizing radiation. The traps are located near the conduction band bottom [29]. The traps are emptied under the action of laser radiation, and electrons locate at deep electron traps. Deep traps are connected with transition metal impurities and antisite defects Nb_{Li} ; they determine photorefractive effect manifestation. It is important to obtain LN crystals with a fast response

to laser radiation, as the magnitude and rate of change in the opening angle of the PILS indicatrix determine the sensitivity and speed of information recording, and the speed of electro-optical modulators and shutters. Thus, such crystals can be used as materials for optical holography, electro-optical modulators, and shutters.

In conclusion, we should say that all found effects were observed after the studied crystals reached the dose of saturation of the radiation color. In addition, we did not find differences in action of β - and γ radiation on LN crystals. This is probably because any ionizing radiation excites interband electrons, recharges charged ions, and creates small-radii polarons based on antisite defects Nb_{Li} . The equivalent action of β - and γ radiation on the LN crystals optical absorption is confirmed by the work [22].

4. Conclusions

A possibility of radiation modification of optical characteristics is shown for $\text{LiNbO}_3\text{:Zn}$ and $\text{LiNbO}_3\text{:Mg}$ crystals. The modification is based on radiation annealing or generation of charged structure defects. The exact manifestation of radiation modification depends only on $\text{LiNbO}_3\text{:Zn}$ crystal dopant concentration.

Due to current scientific data, the treatment of LiNbO_3 crystals with ionizing radiation worsens their optical quality and increases their photorefractive sensitivity. We establish that radiation annealing of defects can improve the optical characteristics of doped $\text{LiNbO}_3\text{:Zn}$ and $\text{LiNbO}_3\text{:Mg}$ crystals. For example, ionizing radiation treatment of below-threshold $\text{LiNbO}_3\text{:Zn}$ crystals ($[\text{ZnO}] \approx 1\text{--}3\text{ mol\%}$) leads to a suppression of photorefractive effect. Ionizing radiation treatment of above-threshold $\text{LiNbO}_3\text{:Zn}$ and $\text{LiNbO}_3\text{:Mg}$ crystals ($[\text{ZnO}] > 5.2\text{ mol\%}$ and $[\text{MgO}] > 5.5\text{ mol\%}$) increases their general optical uniformity. The paper describes the influence of radiation annealing on photorefractive dynamics in weakly doped $\text{LiNbO}_3\text{:Zn}$ crystals ($[\text{ZnO}] \approx 0.04\text{--}0.2\text{ mol\%}$). This knowledge widens the possibilities of application of such crystals as materials for optical holography, electrooptical modulators, and shutters.

Author Contributions: Conceptualization, N.S., M.P. and S.P.; methodology, N.S., M.P. and S.P.; software, S.P.; formal analysis, S.P.; investigation, S.P., N.S. and N.T.; resources, N.S. and M.P.; data curation, S.P., O.M. and N.T.; writing—original draft preparation, S.P., M.P. and N.T.; writing—review and editing, M.P.; visualization, O.M. and N.T.; supervision, N.S. All authors have read and agreed to the published version of the manuscript.

Funding: This work was supported by the Ministry of Science and Higher Education Russian Federation scientific topic No FMEZ-2022-0016.

Data Availability Statement: The raw data required to reproduce these findings are available from corresponding author N.S. on a reasonable request.

Conflicts of Interest: The authors declare no conflict of interest.

References

1. Prokhorov, A.M.; Kuz'minov, Y.S. *Physics and Chemistry of Crystalline Lithium Niobate*; Adam Hilger: New York, NY, USA, 1990; p. 237.
2. Abrahams, S.C.; Levinstein, H.J.; Reddy, J.M. Ferroelectric lithium niobate polycrystal x-ray diffraction study between 24 and 1200 °C. *J. Phys. Chem. Solids* **1966**, *27*, 1019–1026. [[CrossRef](#)]
3. Rauber, A. *Chemistry and Physics of Lithium Niobate. Current Topic in Materials Science*; North-Holland: Amsterdam, The Netherlands, 1978; p. 481.
4. Abrahams, S.C. *Properties of Lithium Niobate*; EMIS Datareviews Series No. 5; The Institution of Engineers: London, UK, 1989; p. 234.
5. Gunter, P.; Huignard, J.P. *Photorefractive Materials and Their Applications. Part 1*; Springer: Berlin, Germany, 2006; p. 243.
6. Volk, T.; Wohlecke, M. *Lithium Niobate. Defects, Photorefractive and Ferroelectric Switching*; Springer: Berlin, Germany, 2008; p. 250.
7. Lengyel, K.; Péter, Á.; Kovacs, L.; Corradi, G.; Palfalvi, L.; Hebling, J.; Unferdorben, M.; Dravec, G.; Hajdara, I.; Szaller, Z.; et al. Growth, defect structure, and THz application of stoichiometric lithium niobate. *Appl. Phys. Rev.* **2015**, *2*, 040601. [[CrossRef](#)]
8. Kong, Y.; Liu, S.; Zhao, Y.; Liu, H.; Chen, S.; Xu, J. Highly optical damage resistant crystal: Zirconium-oxide-doped lithium niobate. *Appl. Phys. Lett.* **2007**, *91*, 081908. [[CrossRef](#)]
9. Xin, F.; Zhang, G.; Bo, F.; Sun, H.; Kong, Y.; Xu, J.; Volk, T.; Rubina, N.M. Ultraviolet photorefractive at 325 nm in doped lithium niobate crystals. *J. Appl. Phys.* **2010**, *107*, 033113. [[CrossRef](#)]

10. Kong, Y.; Bo, F.; Wang, W.; Zheng, D.; Liu, H.; Zhang, G.; Rupp, R.; Xu, J. Recent Progress in Lithium Niobate: Optical Damage, Defect Simulation, and On-Chip Devices. *Adv. Mater.* **2019**, *32*, 1806452. [[CrossRef](#)]
11. Xu, J.; Zhang, G.; Li, F.; Zhang, X.; Sun, Q.; Liu, S.; Song, F.; Kong, Y.; Chen, X.; Qiao, H.; et al. Enhancement of ultraviolet photorefraction in highly magnesium-doped lithium niobate crystals. *Opt. Lett.* **2000**, *25*, 129–131. [[CrossRef](#)]
12. Liu, F.; Kong, Y.; Li, W. High resistance against ultraviolet photorefraction in zirconium-doped lithium niobate crystals. *Opt. Lett.* **2010**, *35*, 10–13. [[CrossRef](#)]
13. Liu, H.; Liang, Q.; Zhu, M.; Li, W.; Liu, S.; Zhang, L.; Chen, S.; Kong, Y.; Xu, J. An excellent crystal for high resistance against optical damage in visible-UV range: Near-stoichiometric zirconium-doped lithium niobate. *Opt. Express.* **2011**, *19*, 1743–1748. [[CrossRef](#)]
14. Kong, T.; Luo, Y.; Wang, W.; Kong, H.; Fan, Z.; Liu, H. Enhanced Ultraviolet Damage Resistance in Magnesium Doped Lithium Niobate Crystals through Zirconium Co-Doping. *Materials* **2021**, *14*, 1017. [[CrossRef](#)]
15. Vartanyan, E.S.; Hovsepian, R.K.; Pogosyan, A.R.; Timofeev, A.L. Influence of γ -irradiation on the photorefractive and photoelectric properties of lithium niobate crystals. *Fiz. Tverd. Tela.* **1984**, *26*, 2418–2423.
16. Orlova, K.N.; Gradoboev, A.V. Radiation resistance of AlGaInP (630 nm) heterostructures with multiple quantum wells. *Izv. Vuzov Fiz.* **2014**, *57*, 63–66.
17. Volk, T.R.; Ivanov, M.A.; Mailman, M.L.; Rubinina, N.M. On the interpretation of radiative optical effects in lithium niobate. *Phys. Tverd. Tela* **1987**, *29*, 871–873.
18. Palatnikov, M.; Sidorov, N.V.; Makarova, O.V.; Manukovskaya, D.V.; Aleshina, L.A.; Kadetova, A.V. Concentration threshold effect on properties of zink-doped lithium niobate crystals. *J. Am. Cer. Soc.* **2017**, *100*, 3703–3711. [[CrossRef](#)]
19. Palatnikov, M.N.; Biryukova, I.V.; Makarova, O.V.; Efremov, V.V.; Kravchenko, O.E.; Skiba, V.I.; Sidorov, N.V.; Efremov, I.N. Growth of heavily doped LiNbO₃:Zn crystals. *Inorg. Mater.* **2015**, *51*, 375–379. [[CrossRef](#)]
20. Palatnikov, M.; Sidorov, N.; Kadetova, A.; Teplyakova, N.; Makarova, O.; Manukovskaya, D. Concentration threshold in optically nonlinear LiNbO₃:Tb crystals. *Opt. Las. Technol.* **2021**, *137*, 106821. [[CrossRef](#)]
21. Palatnikov, M.N.; Sidorov, N.V.; Makarova, O.V.; Efremov, I.N.; Kruk, A.A.; Bormanis, K. The effects of admixtures on resistance to radiation of lithium niobate crystals. *Ferroelectrics* **2015**, *479*, 110–118. [[CrossRef](#)]
22. Palatnikov, M.N.; Sidorov, N.V.; Makarova, O.V.; Panasyuk, S.L.; Kurkamgulova, E.R.; Yudin, I.V. Relationship between the optical damage resistance and radiation hardness and the influence of threshold effects on the radiation hardness of ZnO-doped LiNbO₃ crystals. *Inorg. Mater.* **2018**, *54*, 55–59. [[CrossRef](#)]
23. Mironov, S.P.; Akhmadullin, I.S.; Golenishchev-Kutuzov, V.A.; Migachev, S.A. The optical absorption band of bipolarons in LiNbO₃. *Phys. Sol. St.* **1995**, *37*, 3179–3181.
24. Huixian, F.; Jinke, W.; Huaifu, W.; Shiyang, H.; Yunxia, X. EPR studies of Fe³⁺ in Mg-doped LiNbO₃ crystals. *J. Phys. Chem. Solids* **1990**, *51*, 397–400. [[CrossRef](#)]
25. Kovacs, L.; Corradi, G. New trends in lithium niobate: From bulk to nanocrystals. *Crystals* **2021**, *11*, 1356. [[CrossRef](#)]
26. Schirmer, O.F.; Imlau, M.; Merschjann, C.; Schoke, B. Electron small polarons and bipolarons in LiNbO₃. *J. Phys. Condens. Matter* **2009**, *21*, 123201. [[CrossRef](#)] [[PubMed](#)]
27. Palatnikov, M.; Kadetova, A.; Aleshina, L.; Sidorova, O.; Sidorov, N.; Biryukova, I.; Makarova, O. Growth, structure, physical and chemical characteristics in a series of LiNbO₃:Er crystals of different composition grown in one technological cycle. *Opt. Las. Technol.* **2022**, *147*, 107671. [[CrossRef](#)]
28. Palatnikov, M.; Sidorov, N.; Kadetova, A.; Makarova, O. Growth and concentration dependences of properties of LiNbO₃:Tb crystals grown in a single technological cycle. *Opt. Mater.* **2021**, *122*, 11755. [[CrossRef](#)]
29. Blistanov, A.A.; Lyubchenko, V.M.; Goryunova, A.N. Recombination processes in LiNbO₃ crystals. *Cryst. Rep.* **1998**, *43*, 78–82.